Pharm Res (2014) 31:1032–1045
DOI 10.1007/s11095-013-1225-y

RESEARCH PAPER

Multifunctional Tumor-Targeting Nanocarriers Based on Hyaluronic Acid-Mediated and pH-Sensitive Properties for Efficient Delivery of Docetaxel

Shuangshuang Song • Fen Chen • Huan Qi • Fei Li • Tiegang Xin • Jingwen Xu • Tiantian Ye • Naicheng Sheng • Xinggang Yang • Weisan Pan

Received: 16 June 2013 / Accepted: 3 October 2013 / Published online: 24 October 2013

ABSTRACT

Purpose The objective of this work was to develop a multifunctional tumor-targeting nanocarrier based on the mechanism of CD44-mediated endocytosis and pH-induced drug release to improve the therapeutic efficacy of docetaxel (DTX).

Methods Hyaluronic acid-coated docetaxel-loaded cholesteryl hemisuccinate vesicles (HA-CHEMS vesicles) were prepared. The physiochemical properties and pH-dependent drug release of HA-CHEMS vesicles were evaluated. The HA-CHEMS vesicles were investigated for CD44-mediated internalization and *in vitro* cell viability using MCF-7,A549 and L929 cells.In addition,tissue distribution as well as antitumor efficacy was also evaluated in MCF-7 tumor-bearing mouse model.

Results The particle size and zeta potential of HA-CHEMS vesicles were 131.4 ± 6.2 nm and −13.3 ± 0.04 mV,respectively. The *in vitro* drug release results demonstrated a pH-responsive drug release under different pH conditions. *In vitro* cell viability tests suggested that the encapsulation of DTX in HA-CHEMS vesicles led to more than 51.6-fold and 46.3-fold improved growth inhibition in MCF-7 and A549 cell lines,respectively compared to Taxotere®. From the cell uptake studies,the coumarin 6-loaded HA-CHEMS vesicles enhanced intracellular fluorescent intensity in the CD44-overexpressing cell line (MCF-7). Biodistribution studies revealed selective accumulation of HA-CHEMS vesicles in the MCF-7 bearing BalB/c nude mice as a result of passive accumulation and active targeting (CD44-mediated endocytosis). Compared to Taxotere®,HA-CHEMS vesicles exhibited higher anti-tumor activity by reducing tumor volume ($P < 0.05$) and drug toxicity, demonstrating the success of the multifunctional targeting delivery.

Conclusions This work corresponds to the preparation of a multifunctional tumor-targeted delivery system. Our investigation shows that hyaluronan-bearing docetaxel-loaded cholesteryl hemisuccinate vesicles (HA-CHEMS vesicles) is a highly promising therapeutic system,leading to tumor regression after intravenous administration without visible toxicity.

KEY WORDS CD44 · docetaxel · hyaluronic acid · multifunctional targeting · pH-sensitivity

ABBREVIATIONS

A549	Non small-cell lung cancer
C6	coumarin-6
CHEMS	cholesteryl hemisuccinate
CLSM	confocal laser scanning microscopy
DDAB	dimethyl dioctadecyl ammonium bromide
DL	drug loading
DLS	dynamic light scattering
DMEM	dulbecco's modified Eagle's medium
DTX	docetaxel
EPR	enhanced permeability and retention
EE	encapsulation efficiency
HA	hyaluronic acid hyaluronan
IC_{50}	the growth inhibitory concentration for 50% of the cell population
L929	mice fibroblasts
LYVE-1	the lymphatic vessel endothelial HA receptor-1
MCF-7	human breast cancer cells
MTT	3-(4,5-dimethyl-thiazol-2-yl)-2,5-diphenyl-tetrazolium bromide
MW	molecular weight
PBS	phosphate buffered saline
PI	propidium iodide

S. Song • F. Chen • F. Li • T. Xin • T. Ye • X. Yang • W. Pan (✉)
Department of Pharmaceutics, School of Pharmacy
Shenyang Pharmaceutical University, PO Box No. 122, 103 Wenhua Rd.
Shenyang 110016, People's Republic of China
e-mail: pwstfzy@163.com

H. Qi • J. Xu
Department of Pharmacology and Toxicology, School of Pharmacy
Shenyang Pharmaceutical University, PO Box No. 122, 103 Wenhua Road Shenyang 110016, People's Republic of China

N. Sheng
Insitute of Metal Research, University of Chinese Academy of Sciences
72 Wenhua Road, Shenyang 110016, China

RHMM	receptor for hyaluronate-mediated motility
RPMI	roswell park memorial institute
TEM	transmission electron microscopy
TIR	tumor inhibition rate

INTRODUCTION

Delivering anticancer agents specifically, effectively, and safely to solid tumor remains a significant challenge in recent years. The indiscriminate distribution of anticancer drugs results in potentially toxicity to both normal cells and tumor cells (1,2). The poor clinical outcomes of chemotherapy have promoted the development of targeted drug delivery systems, which increase the delivery of antitumor drugs to the tumor sites and reduce delivery to the normal cells. Hence, an improved therapeutic index can be obtained, contributing to minimizing the severe side effects caused by nonspecific delivery and enhancing tumor-targeting efficacy. Varieties of tumor-targeting mechanisms such as passive targeting *via* EPR effect (3,4), receptor-mediated active targeting (5,6), and environment-sensitive drug controlled release (7,8) have been reported. However, a single targeting strategy is limited to eradicate the tumor because of highly complicated tumor micro-environments (9). Therefore, in this paper, a novel nano drug delivery system was developed for enhancing antitumor efficacy based on a multifunctional targeting strategy: (1) passive targeting by EPR effect, (2) CD44-mediated active targeting, and (3) acidic microenvironment in tumor induced pH-dependent drug release (Scheme 1).

Hyaluronic acid (hyaluronan,HA) is a naturally line polysaccharide composed of repeating disaccharide units of (β,1-4-)-D-glucuronic acid and (β,1-3)-N-acetyl-D-glucosamine, existing in the extracellular matrix and synovial fluids (10,11). HA plays an important role in many biological processes such as proliferation, migration, inflammation and tumor invasion (12,13). HA is potentially very useful in the food, biomedical and cosmetic industries due to its biocompatibility, biodegradability, non-toxicity, and non-immunogenicity (14). In the case of biomedical application, HA has been intensively investigated for site-specific drug delivery to tumor because it has high affinity towards CD44 (the cell adhesion protein family), RHMM (Receptor for hyaluronate-mediated motility) and LYVE-1(the lymphatic vessel endothelial HA receptor-1) (15,16), which are over-expressed in various carcinoma, whereas presenting at lower levels on normal cells. The internalization of HA by cancer cells through CD44 receptors enhances intracellular delivery of drugs *via* conjugation to HA or entrapment in HA modified nanoparticles or micelles (17–20), exhibiting higher therapeutic efficacy compared to the conventional anticancer agents. Thus, HA is a very attractive material as target-specific drug delivery vehicles.

Cholesteryl hemisuccinate (CHEMS) synthesized by succinic acid esterified to the L-hydroxyl group of cholesterol is an acidic cholesterol ester that self-assembles into bilayers in neutral or basic medium. In acidic condition, CHEMS undergoes a phase transformation from stable lamellar phase in neutral pH to the unstable inverted hexagonal phase due to protonation of its acidic head group (21,22). CHEMS is widely applied in the mixtures with surfactants or phospholipids to form pH sensitive vesicles, which are stable in neutral or slight alkaline media, whereas unstable in acidic environment, leading to drug release (23).

Docetaxel (DTX) derived from 10-deacetyl baccatin III (24) is an antineoplastic agent with a broad range of human malignancies. Docetaxel disrupts microtubule dynamics through directly binding to the tubulin, leading to mitotic arrest and eventual apoptosis (25). It is widely used for the treatment of non-small cell lung cancer, locally advanced and metastatic breast cancer, head and neck cancer, prostate cancer and other cancers (26). Docetaxel has a low aqueous solubility of ~6–7 μg/ml. Hence, high concentration of Tween®80 was used to increase solubility of docetaxel (27). Administration of commercial micellar formulation of docetaxel (*i.e.* Taxotere®) is associated with a number of serious side effects due to either the drug itself or the solvent system such as neurotoxicity, hypersensitivity, fluid retention, neutropenia and nail toxicity (28), thus hindering their medical utility for intravenous applications. Furthermore, like most of other conventional chemotherapeutic agents, docetaxel in Taxotere® distributes throughout the body in a nonspecific manner, resulting in a low antitumor activity.

Herein, we hypothesized that the encapsulation of docetaxel into HA-modified CHEMS vesicles as the tumor-targeting delivery system could enhance therapeutic efficacy and reduce the side effects. Upon reaching the tumor tissue by passive and active targeting, HA-modified DTX-loaded CHEMS vesicles would be internalized through interaction between HA and CD44, followed by releasing the drug rapidly in responsive to the lower pH of endosomal/lysosomal compartments (pH 5–6) (29). In this work, the efficacy of HA-modified DTX-loaded CHEMS vesicles as a multifunctional tumor- targeting nano system was investigated both *in vitro* and *in vivo*.

MATERIALS AND METHODS

Reagents and Cell Lines

Docetaxel (DTX) was offered by Jiangsu Hengrui Pharmceutical Co. Ltd. (Jiangsu, China). Sodium hyaluronate (MW = 290 kDa) was purchased from Shandong Freda Biopharm Co. Ltd. (Shandong, China). Cholesteryl hemisuccinate (CHEMS) was synthesized by our own

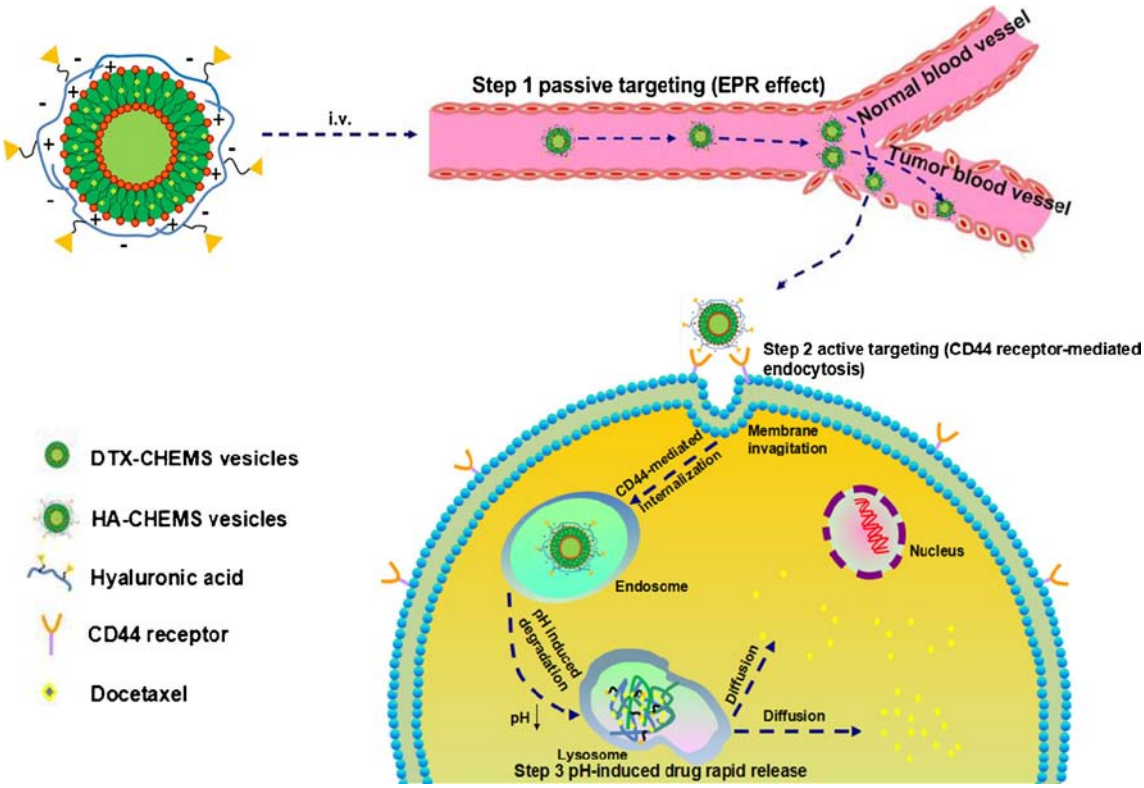

Scheme I Schematic representation of accumulation at tumor tissue and intracellular delivery of HA-CHEMS vesicles.

laboratory. Cholesterol, and succinic anhydride were kindly supplied by China National Medicine Corporation LTD. (Shanghai, China). Coumarin-6, 3-(4, 5-dimethyl-thiazol-2-yl)-2, 5-diphenyl-tetrazolium bromide (MTT) and propidium iodide (PI) were supplied by Sigma–Aldrich Co. (St. Louis, MO, USA). Tween®80 was kindly supplied by AMRESCO LLC(USA). Dimethyl dioctadecyl ammonium bromide (DDAB) was purchased from Tianjin Damao Chemical Reagent Co. (Tianjin, China). Commercial docetaxel solution (Taxotere®) was purchased from Sanofi Aventis (France). All other chemicals and reagents used were of analytical purity grade or higher, obtained commercially.

Dulbecco's modified Eagle's medium (DMEM) and RPMI-1640 were purchased from Gibco (BRL, MD, USA). Human breast cancer cells (MCF-7), non small-cell lung cancer (A549), and mice fibroblasts (L929) were obtained from Chinese Academy of Sciences (Shanghai, China).

Preparation of CHEMS Vesicles Encapsulating DTX (DTX-CHEMS Vesicles)

The DTX-loaded CHEMS vesicles were prepared by a solvent injection method. Briefly, Tween®80 (25 mg), CHEMS (58 mg), DDAB (6.8 mg) and DTX (3.5 mg) were dissolved in 6 ml of chloroform–methanol solvent mixture (2:1, v/v) and added by a micro-syringe into 10 ml of distilled water under vigorous stirring. After injection, the suspension was kept for 30 min at 75°C to evaporate the organic solvent. The residual solvent remaining in the suspension was removed under vacuum at room temperature overnight. The obtained suspension was sonicated at 400 W for 3 min (1 s pulses and 1 s rest, ultrasonic cell crasher). The final concentration of the resultant suspension was 1 mg/ml.

Preparation of Hyaluronic Acid-Coated DTX-CHEMS Vesicles (HA-CHEMS Vesicles)

One milliliter of DTX-loaded CHEMS vesicle suspension was slowly added into an appropriate portion of hyaluronic acid solution at different concentration followed by magnetic agitation at 25°C for 1 h. The effect of the molecular weight of HA, the volume ratio of DTX-loaded CHEMS vesicle suspension to HA solution, the HA concentration on physicochemical properties of HA-CHEMS vesicles was investigated.

Measurement of Drug Loading Content (DL) and Encapsulation Efficiency (EE)

DTX-CHEMS or HA-CHEMS vesicles were separated from the unentrapped drug using a Sephadex G-50 column (2.5 cm×1.0 cm). Briefly, Sephadex G-50 soaked in 100°C distilled water for a few hours was loaded into a 2.5 ml syringe and then centrifugated at 2,000 rpm for 2 min to obtain a dehydrated column. Subsequently, 0.2 ml of vesicle

suspension was added onto the column and centrifugated (2, 000 rpm, 2 min). Afterwards, the column was washed 4 times with 0.2 ml of distilled water each time. After centrifugation, the eluant was collected and destroyed using a mixed solvent of methanol and acetonitrile (1:3). The amount of encapsulated DTX was determined by HPLC. HPLC conditions were as follows: a Diamasil® C18 column (200 mm×4.6 mm, 5 μm, Dikma, China) was used. The mobile phase consisted of acetonitrile and water (62:38, v/v). The flow rate was 1.0 ml/min.

The wavelength was set at 228 nm. In order to determine the total amount of DTX initially added, 0.2 ml of vesicle suspension was destroyed with methanol and acetonitrile and assessed by HPLC. EE and DL were calculated according to the following equations:

$$\mathrm{EE}(\%) = \frac{\text{Weight of the drug in vesicles}}{\text{Weight of the feeding drug}} \times 100$$

$$\mathrm{DL}(\%) = \frac{\text{Weight of the drug in vesicles}}{\text{Weight of the vesicles}} \times 100$$

Characterization of DTX-CHEMS and HA-CHEMS Vesicles

Transmission Electron Microscopy (TEM)

The microstructure of DTX-CHEMS and HA-CHEMS vesicles was observed under the TEM (JEM-1200EX, JEOL, Tokyo, Japan). A drop of vesicle suspension which was diluted 50 fold with double-distilled water was placed onto a carbon film covered with a copper grid and was stained with a drop of 1% (w/v) phosphotungstic acid. Then the sample was dried in the air before TEM observation.

Particle Size and Zeta Potential

The particle size, distribution and zeta potential were determined by dynamic light scattering (DLS) analysis using a zeta potential/particle size analyzer (Malvern Instruments, Malvern, UK). The vesicles were diluted with distilled water prior to analysis, and each experimental result was an average of at least three independent measurements.

Colloidal Stability of DTX-CHEMS and HA-CHEMS Vesicles in PBS and Plasma

The stability of DTX-CHEMS and HA-CHEMS vesicles when dispersed in PBS (pH 7.4) or rat plasma was evaluated by measuring the time-dependent changes in particle size of vesicle suspension. Briefly, 1 ml of vesicle suspension was added to 5 ml of PBS (pH 7.4) or rat plasma and the samples were incubated at 37°C with gentle stirring for 24 h. At different time points, the particle size of vesicles was measured using a zeta potential/particle size analyzer.

In Vitro Drug Release and Evaluation of pH Sensitivity

The dialysis bag diffusion method was applied to investigate the *in vitro* release of DTX from different DTX formulations (30). 3 ml of each of different DTX formulations was placed into a pretreated dialysis bag (MWCO: 8–10 kDa) and incubated in 100 ml of phosphate buffered saline (PBS) of varying pH values ranging from 7.4 to 5.0 containing 0.5% (w/v) Tween®80 at 37 ± 0.5°C with gentle shaking. At predetermined time intervals, 100 μl aliquots of release medium was withdrawn and replaced with an equivalent volume of fresh medium. The samples were centrifugated at 8,000 rpm for 10 min. The concentration of DTX was determined by HPLC as described above. In order to measure the total concentration (corresponding to 100% release), 1 ml of acetonitrile was added into 10 μl of vesicle suspension followed by votex and centrifugation. The obtained supernatant was analyzed by HPLC. The cumulative drug release (%) was plotted as a function of time. Data obtained in triplicate were analyzed graphically.

In Vitro Biological Characterization

Cell Culture

MCF-7, A549 cell lines (high CD44 expression) and L929 cell lines (low CD44 expression) were cultured in DMEM (MCF-7and L929) or RPMI 1640 (A549) medium supplemented with 10% (v/v) fetal bovine serum,100 IU/ml penicillin and 100 g/ml streptomycin at 37°C in a humidified 5% CO^2 atmosphere.

In Vitro Cell Viability

MTT assay was used to evaluate the cell viability of MCF-7, A549 cancer cells and L929 normal cells incubated with different DTX formulations and blank CHEMS vesicles. . Briefly, MCF-7, A549 and L929 cells were seeded in a multiwell-96 plate at the density of 1×10^5 cells per well. After 24 h, the medium was removed and the wells were washed twice with cold PBS. Following that, the cells were incubated with various concentrations of DTX formulations and blank vesicles for 72 h. Four wells for untreated cells and medium were prepared as controls. Then 20 μl of MTT solution (5 mg/ml) was added to each well and incubated for another 4 h at 37°C. Finally, MTT in medium was removed and 200 μl of DMSO was added into each well to dissolve the formazan crystals. Absorbance was measured at 570 nm using a BioRed microplate reader (Model 500, USA). Cell viability was determined by the following formula:

$$\text{Cell viability}(\%) = \frac{\text{Abs(sample)}}{\text{Abs(control)}} \times 100$$

The growth inhibitory concentration for 50% of the cell population (IC_{50}) which can indirectly reflect the cytotoxicity of different DTX formulations was calculated by regression (curve fitting) of the cell viability data. Furthermore, the morphology of cells incubated with different DTX formulations were observed using a microscope system.

Cellular Uptake Studies

The cellular uptake efficiency of different DTX formulations was evaluated by CLSM. The insoluble fluorescent dye coumarin-6 (C6) was loaded into CHEMS vesicles with the same DTX loading method. MCF-7 cells or L929 cells were seeded onto glass coverslips, placed into a 6-well plate, and grown overnight at 37°C in a humidified 5% CO^2 atmosphere. After cell attachment, the medium was replaced with serum-free culture medium containing the free C6 and C6-loaded vesicles (the C6 concentration was 10 μg/ml), respectively, followed by incubation for 2 h. After that, the cells were washed thrice with cold PBS and fixed with 4% paraformaldehyde solution for 10 min. Then, the cells were washed twice with cold PBS. The nuclei were stained by propidium iodide (PI, Sigma) for another 30 min. The fixed cell monolayer was finally washed thrice with PBS. The coverslips were placed onto the glass microscope slides and visualized by a confocal laser scanning microscopy (CLSM, LSM780,Carl Zeiss,Germany). In addition, the cellular uptake mechanism was investigated by the blocking test using free HA (10 mg/ml), negative control of L929 cells, and cell uptake experiment at 4°C.

In Vivo Biological Evaluation

Chromatography

HPLC system was applied to analyze drug concentration of tissue samples. A Promosil C18 column (250 mm × 4.6 mm, 5 μm, Agilent, China) was used. The mobile phase was acetonitrile and water (55:45, v/v). The wavelength was 230 nm and the flow rate was set at 1 ml/min.

Tissue Distribution

All animal experiments were carried out under Shenyang Pharmaceutical University Bioethics Committee Rules and in compliance with Principles of Laboratory Animal Care of national laws. BalB/c nude mice weighing 26–28 g, at the age of 6–8 weeks were used for the study. The MCF-7 cell suspension (2×10^6 cells in 0.2 ml of cell culture medium) was injected subcutaneously into the armpit region to generate the tumor xenograft mouse model. The tumor size was measured by a vernier caliper, and the tumor volume (mm^3) was calculated using the formula $V = 0.5 \times \text{longest diameter} \times \text{shortest diameter}^2$. When the tumor volume reached about 500 mm^3,MCF-7-bearing mice were randomly and equally divided into three groups of 9 mice each: (1) the Taxotere® group, (2) the DTX-CHEMS group, and (3) the HA-CHEMS group. Each group was injected intravenously with the above formulations at a dose of 12 mg/kg through the tail vein. The mice ($n = 3$ per time point) were euthanized by cervical dislocation at predetermined time points (0.5, 2, 6 h), and then the tumor, heart, liver, spleen, lung and kidney were collected, washed, weighed and homogenized in physiological saline at a concentration of 1 g/ml. Afterwards, tissue homogenate was stored at −20°C until further analysis. DTX was extracted from the tissue homogenate by deproteinization using acetonitrile. Briefly, 10 μl of paclitaxel solution (40 μg/ml) as the internal standard was added to 200 μl of tissue sample, and the mixture was extracted with 1 ml of acetonitrile for 10 min followed by centrifugation for 15 min at 12,000 rpm. The supernatant was dried under reduced pressure and redissolved with 100 μl of acetonitrile for HPLC analysis as described above.

In Vivo Antitumor Efficacy

When the tumor volume reached 50–100 mm^3 (24), BalB/c nude mice ($n = 6$/group) bearing subcutaneous MCF-7 tumor were administrated intravenously every 3 days with saline, blank vesicles, Taxotere® with or without DTX, DTX-CHEMS vesicles and HA-CHEMS vesicles for 3 weeks at a dose of 12 mg DTX/kg, respectively. Meanwhile, the tumor volumes and body weights were monitored. After 20 days' observation, tumors were excised from the sacrificed BalB/c nude mice and weighed. Tumor inhibitory rate (TIR) was calculated using the following formula:

$$\text{TIR}(\%) = \frac{W_{\text{control}} - W_{\text{sample}}}{W_{\text{sample}}} \times 100$$

Statistical Analysis

Results were given as mean ± standard deviation (S.D). Both ANOVA and Student's two-sample t-test were utilized for statistical evaluation. Differences were considered significant at a level of $P < 0.05$.

RESULTS AND DISCUSSION

Preparation and Characterization of DTX-CHEMS and HA-CHEMS Vesicles

CHEMS vesicles entrapping DTX were successfully prepared and morphologically spherical vesicles with a smooth surface as revealed by TEM study (Fig. 1a). The existence of HA coating

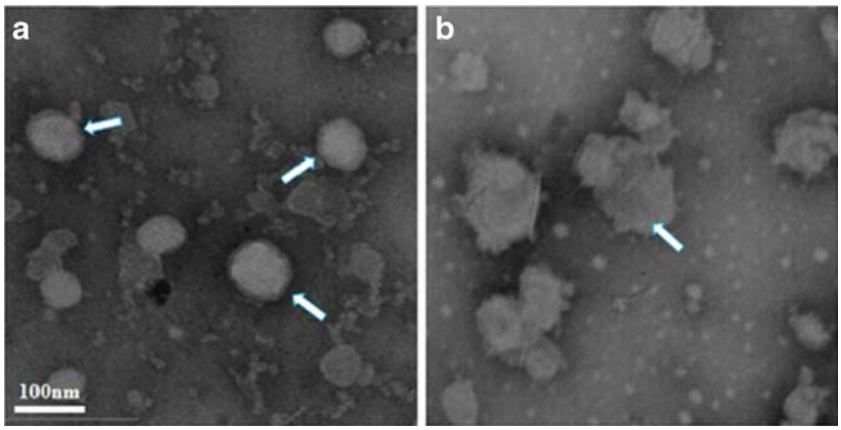

Fig. 1 Transmission electron micrographs of DTX-CHEMS vesicles (**a**) and HA-CHEMS vesicles (**b**).

layer on the surface of CHEMS vesicles was confirmed by the changes in particle size, zeta potential and morphology observed by TEM (Fig. 1b). As shown in Table I, the encapsulation efficiency was determined to be 92.5±1.4% and 91.4±1.7% in DTX-CHEMS vesicles and HA-CHEMS vesicles, respectively, which suggested the existence of coating layers had no effect on encapsulation efficiency. The mean particle size of vesicles was 65.9±3.2 nm and 131.4±6.2 nm for DTX-CHEMS vesicles and HA- CHEMS vesicles with distinct difference in particle size. DTX-CHEMS vesicles showed a positive zeta potential. However, the coating of vesicles by hyaluronic acid converted the zeta potential from positive to negative values.

The colloidal stability in plasma conferred increased importance to the preclinical study of nanoenabled drug delivery systerms. Therefore the *in vitro* colloidal stability of vesicles was evaluated in PBS (pH 7.4) and rat plasma (Fig. 2). In PBS, both of the vesicles were stable with no significant size change for HA-CHEMS vesicles and a slight increase in particle size for DTX-CHEMS vesicles. When incubated in human plasma, the particle size of HA-CHEMS vesicles increased to about 1.3-fold of the original size, while the particle size for the DTX-CHEMS vesicles rapidly increased to 4.2-fold over the 24 h incubation. From the incubation picture, it can be seen that HA-CHEMS vesicle dispersion was clear with the absence of any precipitate at different incubation time. However, in the case of DTX-CHEMS vesicles, there appeared visible floccule after 24 h incubation. Our results highlighted the enhanced stability of HA-CHEMS vesicles in rat plasma compared to uncoated DTX-CHEMS vesicles. Since the experiment in the present work was not able to ascertain whether all of the vesicles were intact upon incubation with plasma, further investigation will be needed.

Effects of HA Coating on Characteristics of DTX-CHEMS Vesicles

The particle size and zeta potential are the important parameter for HA-coated vesicles from pharmaceutical viewpoint. HA-coated vesicles with proper particle size and zeta potential will contribute to improve the *in vitro* stability and the *in vivo* targeting. As a result, we investigated the effects of HA concentration, volume ratio of vesicle suspension to HA solution and molecular weight of HA on the physicochemical properties of HA- CHEMS vesicles.

Effect of HA Concentration

A series of DTX-CHEMS vesicles coated with different concentration of HA was prepared at the fixed volume ratio (1/1, 1/2) and molecular weight of HA (290 kDa). HA concentration was found to have a significant effect on the particle size and zeta potential of HA-CHEMS vesicles (Fig. 3). When the volume ratio was fixed at 1/1, the particle size and zeta potential of HA- CHEMS vesicles significantly decreased ($P<0.05$) from 1020.1 to 185.2 nm and from +0.2 to −10.5 mV for the particle size and zeta potential, respectively, with HA concentration increasing from 0.1% to 0.2% (w/v). However, further increase in HA concentration from 0.2% to 0.3% showed an increase in particle size. This might be explained that as the increase of HA concentration, more and more HA molecular anchored on the surface of vesicles, which led to sufficient negative charge needed to stabilize vesicles. At HA concentration ≤0.1%, bridging or depletion flocculation occurred amongvesicles, resulting in the larger particle size. As the HA concentration increased to 0.3%, there was no significant

Table I The Physicochemical Characterization and Drug Loading Parameters of DTX-CHEMS Vesicles and HA-CHEMS Vesicles

Formulations	Particle size (nm)	Polydispersity index	Zeta potential (mV)	DL (%)	EE (%)
DTX-CHEMS	65.9±3.2	0.132±0.021	11.8±0.2	3.38±0.05	92.5±1.4
HA-CHEMS	131.4±6.2	0.232±0.036	−13.3±0.4	3.44±0.07	91.4±1.7

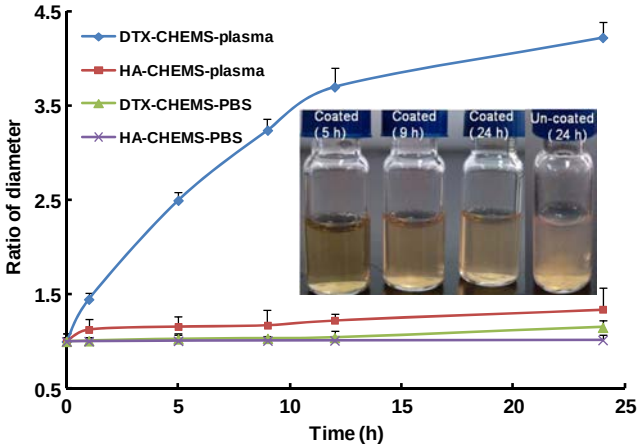

Fig. 2 The colloidal stability of HA-CHEMS and DTX-CHEMS vesicles in PBS (pH7.4) and rat plasma for 24 h. The ratio of diameter was the ratio of time-dependent particle size to original particle size. Inset: photographs of HA-CHEMS and DTX-CHEMS vesicles after incubation with rat plasma for different time.

difference in terms of particle size and zeta potential compared with thoseof 0.25% HA-coated vesicles. This might be due to the fact that saturation of the coating layer had reached in the presence of 0.25% of HA solution and hence further increase in HA concentration would not change the coating strength and zeta potential of HA- CHEMS vesicles (31). This leads to the assumption that the surface of vesicles could be attached a certain amount of HA but to a maximum limit after which any increase in HA concentration would not significantly influence the physicochemical properties of HA-CHEMS vesicles. Comparing Fig. 3a with Fig. 3b, it could be found that when the total amount of HA was equivalent, the particle size and zeta potential of HA- CHEMS vesicles in the volume ratio of 1/2 were superior to those in the volume ratio of 1:1, suggesting that HA coating on the surface of CHEMS vesicles in low concentration and large volume excelled that in high concentration and small volume at the same amount of HA.

Effect of Molecular Weight of HA

The effect of molecular weight of HA in the range of 35–1, 490 kDa on the particle size and zeta potential of HA-CHEMS vesicles was profiled in Fig. 4. The volume ratio and HA concentration were fixed at 1/2 and 0.1%, respectively. Increasing molecular weight from 35 to 1,490 kDa led to asignificant increase in the particle size of HA- CHEMS vesicles and significant decrease in the zeta potential ($P < 0.05$). This might be attributed to the fact that with the increase of molecular weight of HA, the coating layer on the DTX-CHEMS vesicles is more and more thicker, resulting in the larger vesicles. Moreover, the larger the molecular weight of HA is, the more the number of $-COO^-$ group attached to the backbone of HA is, and hence, the more negative charge is obtained.

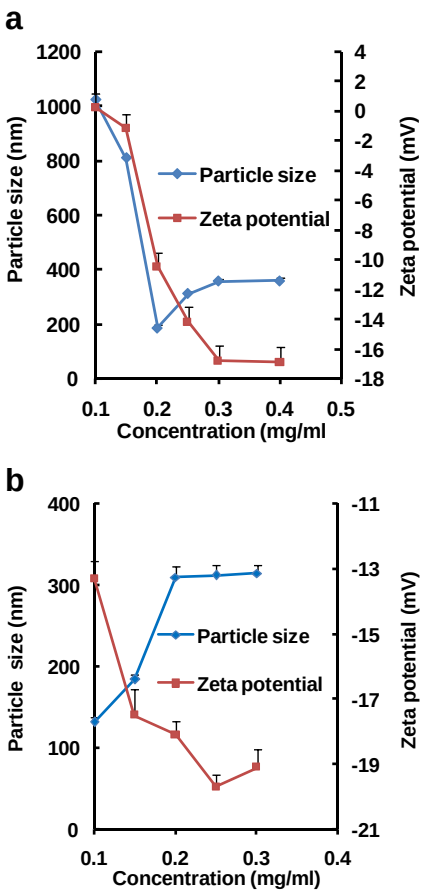

Fig. 3 The effect of HA concentration on particle size and zeta potential. (**a**) The volume ratio of vesicle suspension to HA solution was 1/1. (**b**) The volume ratio of vesicle suspension to HA solution was 1/2.

Effect of Volume Ratio of Vesicle Suspension to HA Solution

Figure 5 shows both zeta potential and particle size of CHEMS vesicles after they were titrated into HA solutions that varied in volume from 1 ml to 3 ml. When the volume of

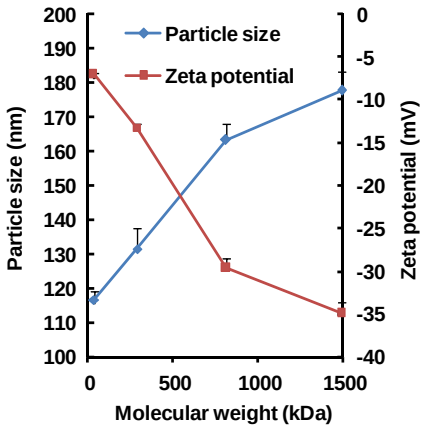

Fig. 4 The effect of molecular weight of HA on particle size and zeta potential. The molecular weight was 35, 290, 840, and 1,490 kDa, respectively.

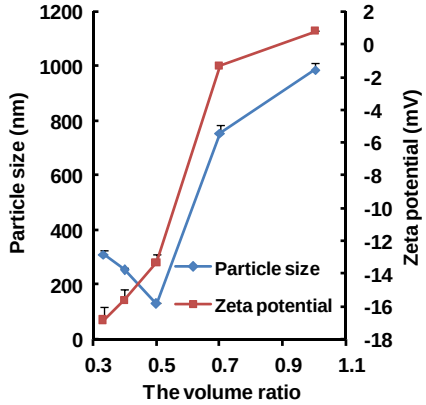

Fig. 5 The effect of volume ratio of vesicle suspension to HA solution on particle size and zeta potential. The volume ratio was set at 1/1, 2/3, 1/2, 2/5 and 1/3, respectively.

HA solution increased, the zeta potential continued to decrease; with respect to the particle size, it initially reduced from 986.4 to 131.4 nm and subsequently increased to 312.4 nm.

In Vitro Drug Release and Preliminary Assessment of pH Sensitivity

In vitro release behavior of Taxotere®, DTX-CHEMS vesicles and HA-CHEMS vesicles was carried out in PBS (pH7.4) containing 0.5%Tween®80 which could improve the solubility of DTX and reach the sink condition. As shown in Fig. 6, both DTX-CHEMS vesicles and HA-CHEMS vesicles showed an initial fast release followed by a plateau and a second release stage. It was obvious that DTX release from DTX-CHEMS vesicles and HA-CHEMS vesicles was much slower than Taxotere® ($P<0.05$). Approximately 100% of DTX from Taxotere® was released within 24 h, whereas the percentage of DTX released from DTX-CHEMS vesicles

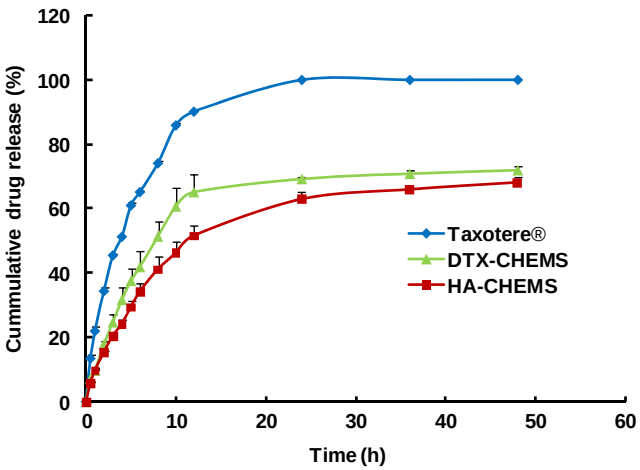

Fig. 6 *In vitro* drug release profiles of Taxotere®, DTX-CHEMS vesicles and HA-CHEMS vesicles. Data were expressed as mean ± S.D. ($n=3$).

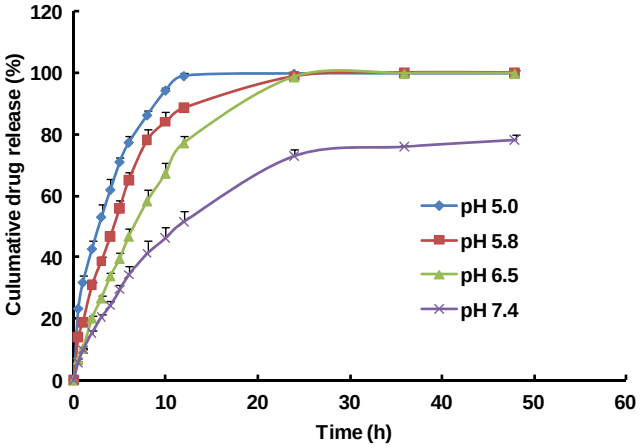

Fig. 7 *In vitro* drug release of DTX-CHEMS vesicles coated with hyaluronic acid (290 kDa) at different pH. Data represented mean ± S.D. ($n=3$).

and HA-CHEMS vesicles was 69.4% and 62.9%, respectively. From Fig. 6, we could also observe that there was a significant ($P<0.05$) decrease in the *in vitro* drug release from HA-coated CHEMS vesicles compared with uncoated CHEMS vesicles (DTX-CHEMS). The slower release rate of HA-CHEMS vesicles might be caused by the coating layer surrounding the vesicles, which blocked the drug release from the interior of vesicles.

Different DTX formulations were subjected to the changes in pH. The extent of DTX release in PBS with different pH was determined. Results were summarized in Figs. 7 and 8. The *in vitro* cumulative release of DTX from HA-coated CHEMS vesicles increased dramatically when lowering the pH. About 71.1%, 57.9% and 39.5% of DTX was released at pH 5.0, 5.8 and 6.5 after 5 h, respectively, while the percentage of release was 29.5% at pH 7.4. Furthermore, most of the encapsulated drug was released from HA-coated CHEMS vesicles within 12 h at pH 5.0 and 5.8. It can be seen in Fig. 8 that the accumulative release of free drug solution and

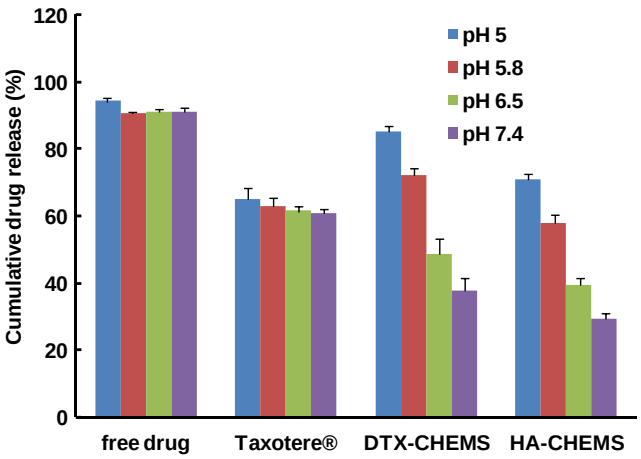

Fig. 8 The cumulative release pencentage of free drug in 50% ethanol, Taxotere®, DTX-CHEMS vesicles and HA-CHEMS vesicles at different pH after 5 h. Data were expressed as mean ± S.D. ($n=3$).

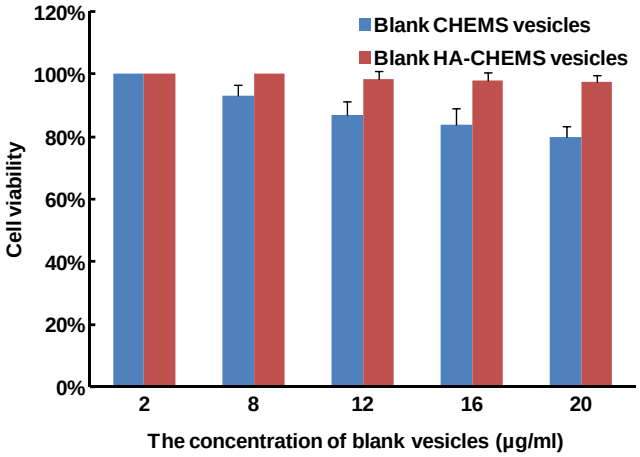

Fig. 9 *In vitro* cell viability of blank CHEMS vesicles and blank HA-CHEMS vesicles against MCF-7 cells (mean ± S.D., $n = 3$).

Taxotere® had no significant difference at all pH tested ($P > 0.1$). However, nude CHEMS vesicles and HA-coated CHEMS vesicles displayed distinct pH-dependence ($P < 0.05$). So we can conclude that indeed, it is CHEMS that triggers the leakage of encapsulated DTX through the vesicle membrane. In neutral or alkaline aqueous media, CHEMS adopts a lamellar organization in vesicles, whereas at acidic pH, because of protonation of the $-COO^-$ group of CHEMS, it displays a hexagonal phase (32). This structure is unstable, contributing to the pH sensitive fusion of vesicles, and hence resulting in fast leakage of DTX. The results suggested that the property of sustained release in the normal physiological media and accelerating release in the acidic environment would be useful for improving the anticancer activity.

In Vitro Biological Characterization

In Vitro Cell Viability

MTT assay used in this paper is a cell viability assay often used to determine cytotoxicity following exposure to toxic substances. The cell viability of blank vesicles and various DTX formulations against MCF-7, A549 and L929 cell lines were evaluated. The results of cell viability after addition of blank vesicles were shown in Fig. 9. The viabilities (%) were over 80% at all concentrations (1–20 μg/ml) tested in the three cell lines (the data of A549 and L929 cell lines not shown). According to the relationship between the relative growth rate and the cytotoxicity grade, the cytotoxicity of blank vesicles at all concentrations were all grade 0 and 1(33,34). This indicated that blank vesicles displayed no significant cytotoxicity to carcinomatous or normal cells. We could also find that blank HA-CHEMS vesicles showed a better cell viabilities, implying that the coating of HA on the surface of vesicles reduced the contact of Tween®80 with cell membrane. The values of IC_{50} of DTX entrapped in HA-coated CHEMS vesicles, naked CHEMS vesicles and Taxotere® were summarized in Table II. It was found that the DTX-loaded vesicles induced cell growth inhibition more forcefully compared with commercial Taxotere® in an equivalent drug concentration level applied. The IC_{50} of HA-coated CHEMS vesicles was 14.33 ± 2.55 ng/ml to MCF-7 cells and 7.23 ± 0.25 ng/ml to A549 cells, which was 51.6-fold and 46.3-fold higher than that of Taxotere®, respectively. That is to say, the HA-coated DTX-loaded CHEMS vesicles caused a potent anticancer activity already at lower DTX dosages. The value of potentiating factor (PF) was defined as the ratio of the IC_{50} of DTX entrapped in vesicles to the IC_{50} of Taxotere® (35). The obtained data showed that the PF values of DTX-CHEMS vesicles and HA-CHEMS vesicles were both higher than 1.0 in the cancer cell lines used for the tests, indicating that DTX-loaded vesicles potentiated the growth inhibition induced by Taxotere®. Furthermore, we observed that the $IC_{50}$of HA-CHEMS vesicles to cancer cell lines was far lower than that to normal cells compared with Taxotere® and DTX-CHEMS vesicles, implying that HA-CHEMS vesicles exhibited a higher selectivity and cytotoxicity to carcinomatous cell lines. The morphology of cells exposed to different DTX formulations for 72 h was also observed (Fig. 10). It can be seen that most of MCF-7 and A549 cells treated with HA-CHEMS vesicles exhibited the apoptotic morphology.

Cell Uptake Studies

To investigate the cellular uptake mechanism of CHEMS vesiclesMCF-7 cells and L929 cells incubated with C6-loaded vesicles were observed by CLSM. Because of the similar results in MCF-7 and A549 cell lines, we only displayed the images of MCF-7 cells. In order to better compare the intensity of fluorescence among the cells treated with C6 solution and C6-loaded vesicles, the images were taken under the same imaging parameters throughout the cell imaging process. As presented in Fig. 11, the images obtained from the FITC channel showed the green fluorescence of C6

Table II Cytotoxicity of DTX Formulations Against Carcinomatous and Normal Cell Lines, Expressed as IC_{50} Values

Cell lines	Taxotere® (ng/ml)	DTX-CHEMS (ng/ml)	PF	HA-CHEMS (ng/ml)	PF
MCF-7	723.66 ± 3.68	248.14 ± 4.89	2.9	14.33 ± 2.55	51.6
A549	324.33 ± 6.03	237.33 ± 5.03	1.4	7.23 ± 0.25	46.3
L929	479.00 ± 3.27	366.04 ± 3.32	–	175.33 ± 3.68	–

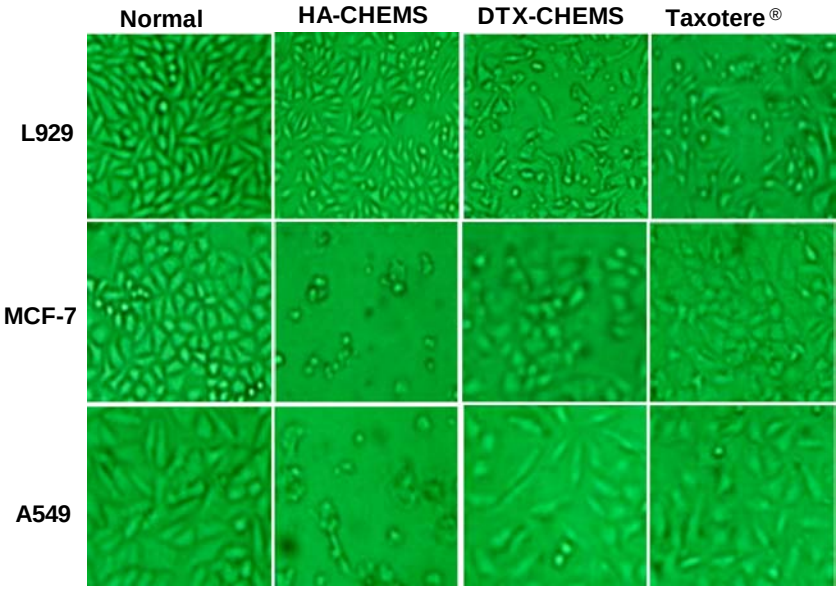

Fig. 10 The pictures of MCF-7, A549 and L929 cells incubated with different DTX formulations at DTX concentration of 0.04 μg/mL for 72 h. The magnification was 10× 25.

and the images obtained from the PI channel exhibited the red fluorescence of nuclei. It can be observed that in the merged channel of FITC and PI, fluorescent signals of MCF-7 cells incubated with C6 solution and C6-loaded vesicles at 37°C were all visualized in the cytoplasm. However, fluorescent intensity of MCF-7 cells treated with C6-loaded

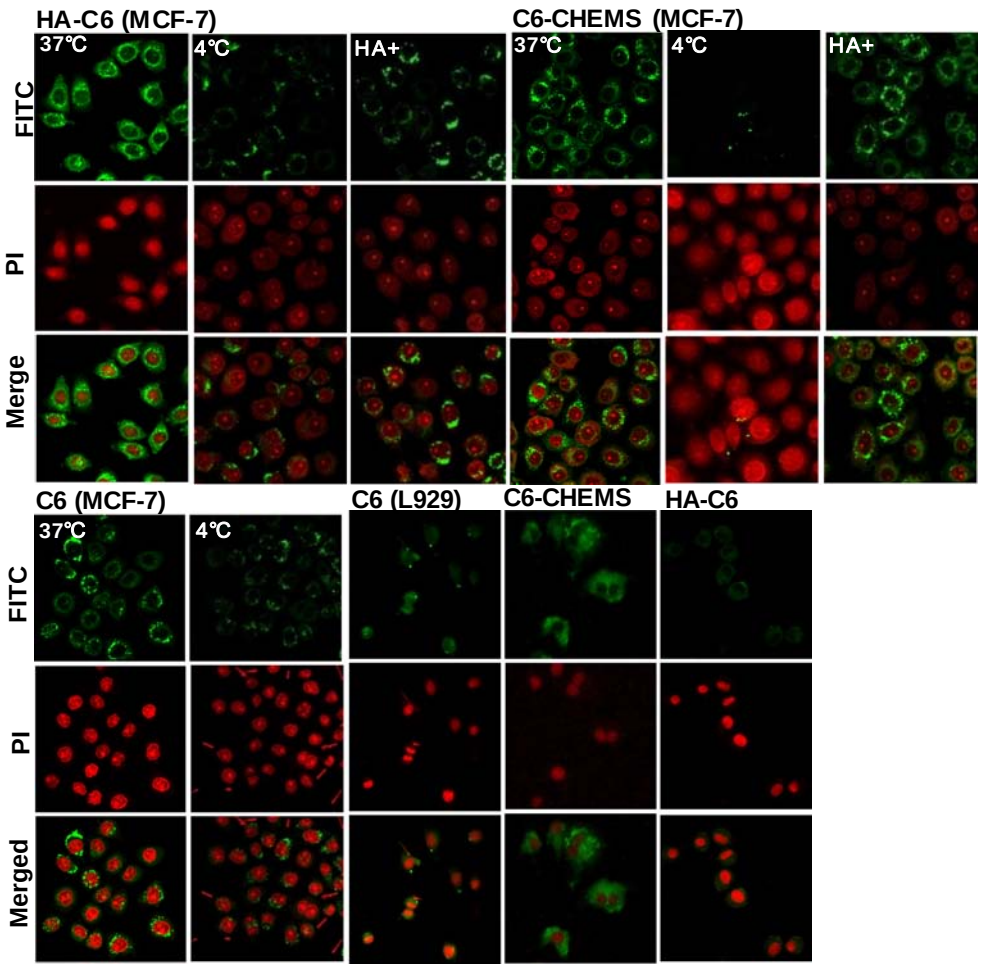

Fig. 11 CLSM of MCF-7 cells and L929 cells incubated with free coumarin-6, coumarin-6-loaded CHEMS vesicles (C6-CHEMS vesicles) and coumarin-6-loaded HA-CHEMS vesicles (C6-HA vesicles) (20×).

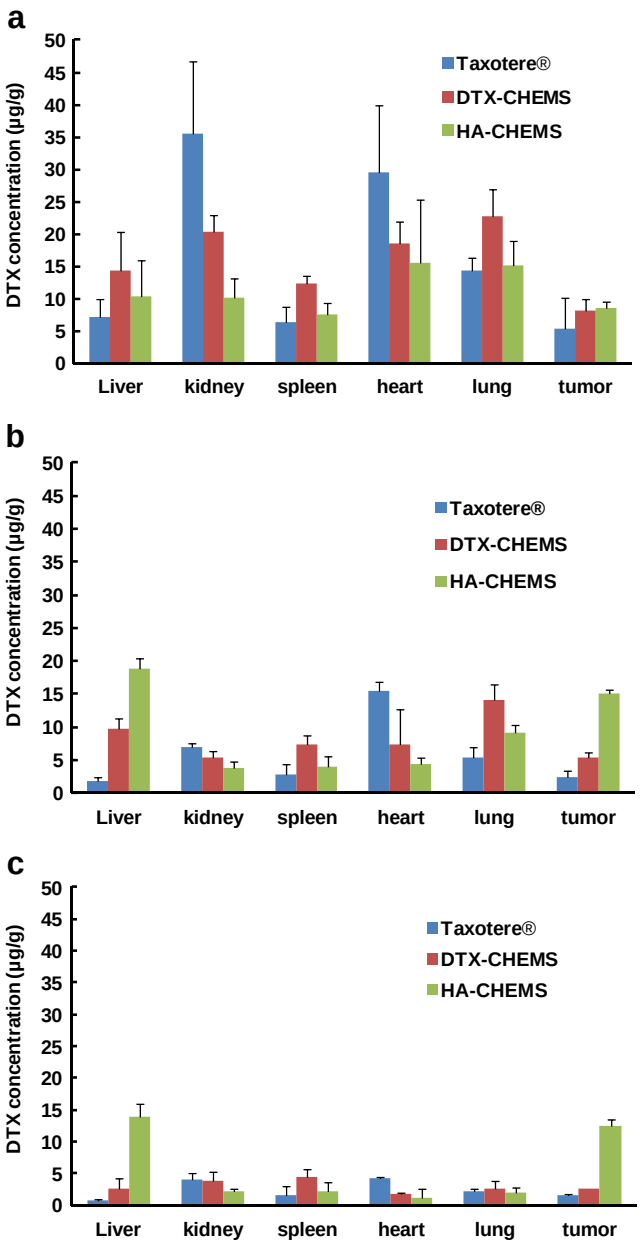

Fig. 12 The mean concentrations of DTX in different tissues of MCF-7 tumor-bearing mice after intravenous administration of Taxotere®, DTX-CHEMS vesicles and HA-CHEMS vesicles at 0.25 h (**a**), 2 h (**b**) and 6 h (**c**) ($n = 3$).

HA-CHEMS vesicles (HA-C6 vesicles) was significantly higher than that treated with nude C6- CHEMS vesicles and C6 solution. As expected, the green fluorescence of C6 solution showed a sparse and asymmetrical accumulation in the cytoplasm; in contrast, the green fluorescence in the MCF-7 cells treated with HA-C6 vesicles was bright and symmetrical. Moreover, cells treated with HA-C6 vesicles showed the obviously increased nuclear and perinuclear fluorescence accumulation compared with C6 solution and nude C6-CHEMS vesicles. When the MCF-7 cells were simultaneously incubated with HA solution (10 mg/ml) and C6-loaded vesicles, the intracellular fluorescent intensity of HA-C6 vesicles was substantially reduced compared to that of HA-C6 vesicles in the HA-free medium; whereas as for the C6-CHEMS vesicles, there was no significant difference in fluorescent intensity. The difference may be explained by the fact that the CD44 receptor was blocked by the HA solution, leading to the decreased cell uptake of HA-C6 vesicles. In L929 cells (low expression of CD44), as for HA-C6 vesicles, the fluorescent signal was weaker than that of MCF-7 cells treated with HA-C6 vesicles due to low CD44 expression; however, the fluorescent intensity of C6 solution and C6-CHEMS vesicles in MCF-7 cells and L929 cells was no significant difference. In addition, we can also find that the cell uptake of C6-CHEMS vesicles and HA-C6 vesicles was an energy-dependent process, as evidenced by the reduction in fluorescent intensity at 4°C. The fluorescent signal was hardly observed for the C6-CHEMS vesicles. In contrast, the fluorescent intensity of C6 solution was not largely inhibited possibly because of passive diffusion. These results demonstrated that HA-CHEMS vesicles can specifically bind to CD44 and internalize into cancer cells *via* CD44 receptor-mediated endocytosis.

In Vivo Biological Evaluation

Tissue Distribution

To verify specifically target of HA-CHEMS vesicles to carcinoma xenografts *in vivo*, the tissue distribution of DTX in different formulations was evaluated in the MCF-7 tumor-bearing mouse model. The biodistribution patterns of HA-CHEMS vesicles, DTX-CHEMS vesicles and Taxotere® in main organs and tumors were presented in Fig. 12. The obtained results showed that the concentration of DTX from

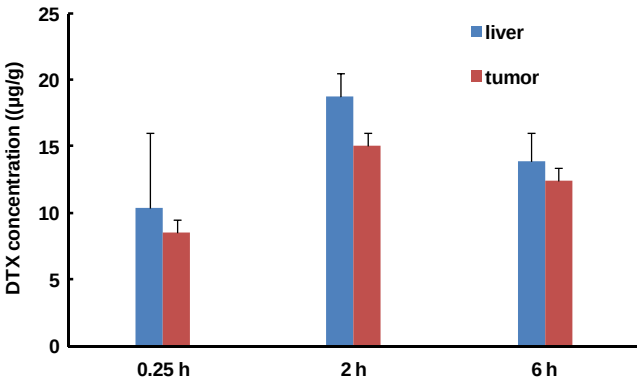

Fig. 13 The distribution of DTX in liver and tumor after i.v. of HA-CHEMS vesicles to MCF-7 tumor-bearing mice at 0.25, 2 and 6 h. The data were presented as mean ± S.D. ($n = 3$).

Taxotere® in heart and kidney was higher than that from DTX-CHEMS vesicles and HA-CHEMS vesicles. This indicated Taxotere® had higher toxicity to heart and faster elimination in kidney. It is worthy to note that DTX from DTX-CHEMS vesicles accumulated significantly in liver, lung and spleen. However, It is interesting that there exhibited a decreased accumulation for the HA-CHEMS vesicles in lung and spleen and an increased accumulation in liver compared to DTX-CHEMS vesicles. This may be explained by two reasons (1) the hydroxyl-rich hyaluronan is similar to PEG, contributing to steric stabilization of the vesicles and providing protection from the opsonization, (36,37). (2) It was reported that liver sinusoidal endothelial cells expressed the HARE receptor (38–40), consequently resulting in a higher accumulation in liver compared to DTX-CHEMS vesicles. The tumor accumulation of DTX in different formulations was in the following order at three time points: HA-CHEMS vesicles >DTX-CHEMS vesicles >Taxotere®. Interestingly, compared with DTX-CHEMS vesicles and Taxotere®, HA-CHEMS vesicles increased DTX accumulation in the tumor by 4.8-fold and 8.5-fold, respectively at 6 h post-injection, this may be due to the success of combination of active targeting and passive targeting. In addition, we can also find that the concentration change trend of DTX in liver was consistent with that in tumor (Fig. 13), fully suggesting that receptor-mediated endocytosis played an important role on DTX accumulation in tumor and liver.

In Vivo Antitumor Efficacy

The *in vivo* antitumor activity was evaluated in BalB/c nude mice bearing MCF-7 tumor. In order to investigate the antitumor activity and systemic toxicity of different DTX formulations, the variation in tumor volume and body weight was monitored (Fig. 14). From the Fig. 14a, it can be seen that HA-CHEMS vesicles exhibited the highest tumor growth suppression among all DTX formulations. Blank CHEMS vesicles and blank Taxotere® had no effect on tumor growth, whereas intersetingly, blank HA-CHEMS vesicles showed a slight tumor inhibition, which could further enhance the antitumor

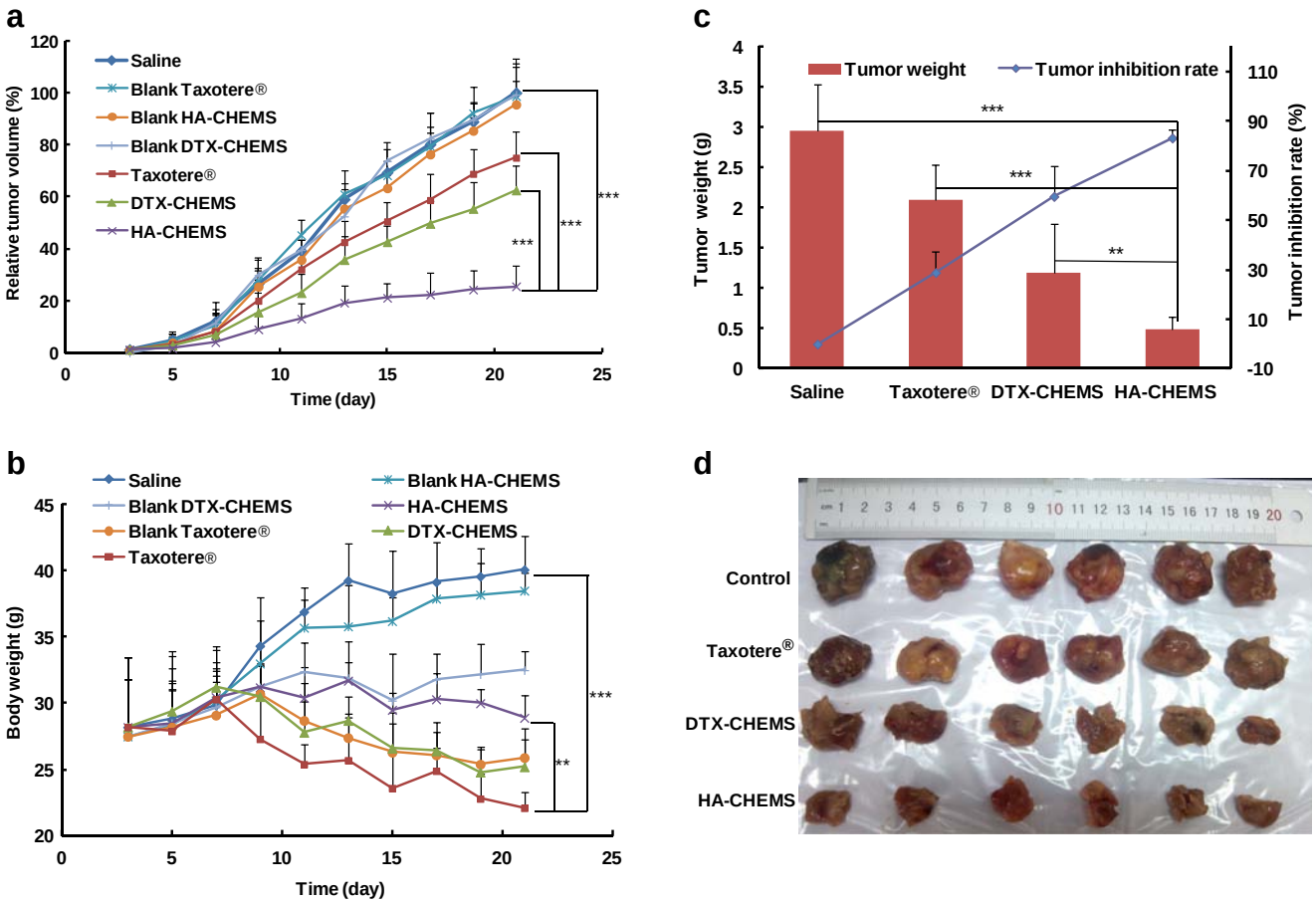

Fig. 14 (**a**) Changes of tumor volume after intravenous injection of saline, blank vesicles, Taxotere® with or without DTX, DTX-CHEMS vesicles and HA-CHEMS vesicles in MCF-7 tumor-bearing nude mice. (**b**) Body weight change of MCF-7-bearing nude mice treated with saline, blank vesicles, Taxotere® with or with DTX, DTX-CHEMS vesicles and HA-CHEMS vesicles. (**c**) Tumor weight and TIR of saline-, Taxotere®-, DTX-CHEMS vesicles- and HA-CHEMS vesicles-treated MCF-7-bearing nude mice at day 21 after the mice were euthanized. (**d**) Photograph of tumors stripped from mice administrated intravenously with saline, Taxotere®, DTX-CHEMS vesicles and HA-CHEMS vesicles. The results were shown as the mean ± S.D. ($n = 6$). *$P < 0.05$. **$P < 0.01$. ***$P < 0.001$.

effect of DTX-loaded HA-CHEMS vesicles. The tumor volumeof mice treated with Taxotere®, DTX-CHEMS vesicles and HA-CHEMS vesicles was 74.8%, 62.5% and 25.3% of the saline-treated mice, respectively after 20 days. As presented in Fig. 14b, the TIR value of HA-CHEMS vesicles was calculated to be 76.4%, which was 1.28-fold and 2.65-fold higher than that of DTX-CHEMS vesicles and Taxotere®, respectively. This indicated that CD44-mediated endocytosis enhanced the therapeutic efficacy of HA-CHEMS vesicles. In the case of variation of body weights (Fig. 14c), the body weight of blank Taxotere®-treated mice decreased significantly. This might be due to repeated injection of high concentration of Tween®80 which induced the toxicity to normal tissue. The increase in body weight of blank HA-CHEMS vesicles-treated mice was higher than that of blank CHEMS vesicles-treated mice, indicating that repeated injection of blank CHEMS vesicles had toxicity to the body possibly because non-selectivity of blank CHEMS vesicles caused accumulation of Tween®80 in normal tissue. the decrease of body weightof mice treated with Taxotere® and DTX-CHEMS vesicles at the end of experiment was up to 21.6% and 10.6% of original weight, respectively, while no significant body weight loss was observed after the administration of HA-CHEMS vesicles, indicating that entrapping DTX into HA-coated CHEMS vesicles could reduce effectively the side effects and toxicity induced by free DTX and Tween®80 . In addition, the tumor image (Fig. 14d) and weight obtained from the sacrificed mice treated with different DTX formulation also demonstrated that HA-CHEMS vesicles showed excellent antitumor activity. The obtained results suggest that the CHEMS vesicles modified with HA have promising potential as targeting carriers for efficient tumor therapy.

CONCLUSIONS

In this study, we successfully prepared hyaluronic acid-coated docetaxel-loaded CHEMS vesicles. And their *in vitro* and *in vivo* performances were evaluated. Compared to commercial Taxotere®, HA-CHEMS vesicles exhibited several advantages including the high selectivity to CD44overexpressing tumor cells, the pH-triggered rapid release of DTX, passive targeting *via* EPR, and the extremely low cytotoxicity to the normal cells or tissues. As a result, the HA-CHEMS vesicles significantly improved the therapeutic efficacy of DTX *in vitro* by at least 51.6-fold and 46.3-fold in MCF-7 and A549 cell lines, respectively compared with commercial Taxotere®. *In vivo* biodistribution studies showed that HA-CHEMS vesicles exhibited 8.5-fold higher accumulation in tumor than Taxorere® at 6 h post-injection. *In vivo* antitumor efficacy confirmed that HA-CHEMS vesicles possessed much higher tumor-targeting capacity than Taxorere® and exhibited enhanced antitumorefficacy and decreased systemic toxicity. These studies provide a proof of principle that hyaluronic acid-coated docetaxel-loaded CHEMS vesicles may be an attractive drug delivery system for anti-tumor therapy, combining efficacy against the tumor with the lowest possible side effects on normal tissues and organs after systemic administration.

ACKNOWLEDGMENTS AND DISCLOSURES

This work was financially supported by the National Natural Science Foundation of China (NSFC,No.81273447), and Heibei Natural Science Foundation of China (HENSF, C2011139007).

REFERENCES

1. Jain RK. Delivery of molecular and cellular medicine to solid tumors. Adv Drug Deliv Rev. 2001;46:149–68.
2. Allenand TM, Cullis PR. Drug delivery systems: entering the mainstream. Science. 2004;303:1818–22.
3. Iyer AK, Khaled G, Fang J, Maeda H. Exploiting the enhanced permeability and retention effect for tumor targeting. Drug Discov Today. 2006;11:812–8.
4. Maeda H, Wu J, Sawa T, Matsumura Y, Hori K. Tumor vascular permeability and the EPR effect in macromolecular therapeutics: a review. J Control Release. 2000;65:271–84.
5. Xiang G, Wu J, Lu Y, Liu Z, Lee RJ. Synthesis and evaluation of a novel ligand for folate-mediated targeting liposomes. Int J Pharm. 2008;356:29–36.
6. Hatakeyama H, Akita H, Maruyama K, Suhara T, Harashima H. Factors governing the in vivo tissue uptake of transferrin-coupled polyethylene glycol liposomes in vivo. Int J Pharm. 2004;281:25–33.
7. Chen Y, Youn P, Furgeson DY. Thermo-targeted drug delivery of geldanamycin to hyperthermic tumor margins with diblock elastin-based biopolymers. J Control Release. 2011;155:175–83.
8. Xu H, Deng Y, Chen D, Hong W, Lu Y, Dong X. Esterase-catalyzed dePEGylation of pH-sensitive vesicles modified with cleavable PEG-lipid derivatives. J Control Release. 2008;130:238–45.
9. Shen M, Huang Y, Han L, Qin J, Fang X, Wang J, *et al*. Multifunctional drug delivery system for targeting tumor and its acidic microenvironment. J Control Release. 2012;161:884–92.
10. Choi KY, Chung H, Min KH, Yoon HY, Kim K, Park JH, *et al*. Self-assembled hyaluronic acid nanoparticles for active tumor targeting. Biomaterials. 2010;31:106–14.
11. Robert L, Robert AM, Renard G. Biological effects of hyaluronan in connective tissues, eye, skin, venous wall. Role in aging. Pathol Biol. 2010;58:187–98.
12. Schanté CE, Zuber G, Herlin C, Vandamme TF. Chemical modifications of hyaluronic acid for the synthesis of derivatives for a broad range of biomedical applications. Carbohydr Polym. 2011;85:469–89.
13. Yin D-S, Z-q G, W-y Y, C-x L, Y-j Y. Inhibition of tumor metastasis in vivo by combination of paclitaxel and hyaluronic acid. Cancer Lett. 2006;243:71–9.
14. Liu Y, Sun J, Cao W, Yang J, Lian H, Li X, *et al*. Dual targeting folate-conjugated hyaluronic acid polymeric micelles for paclitaxel delivery. Int J Pharm. 2011;421:160–9.
15. Orian-Rousseau V. CD44, a therapeutic target for metastasising tumours. Eur J Cancer. 2010;46:1271–7.

16. Journo-Gershfeld G, Kapp D, Shamay Y, Kopeček J, David A. Hyaluronan oligomers-HPMA copolymer conjugates for targeting paclitaxel to CD44-overexpressing ovarian carcinoma. Pharm Res. 2012;29:1121–33.
17. Xin D, Wang Y, Xiang J. The use of amino acid linkers in the conjugation of paclitaxel with hyaluronic acid as drug delivery system: synthesis, self-assembled property, drug release, and in vitro efficiency. Pharm Res. 2010;27:380–9.
18. Upadhyay KK, Bhatt AN, Mishra AK, Dwarakanath BS, Jain S, Schatz C, *et al*. The intracellular drug delivery and anti tumor activity of doxorubicin loaded poly(γ-benzyl l-glutamate)-b-hyaluronan polymersomes. Biomaterials. 2010;31:2882–92.
19. Raviña M, Cubillo E, Olmeda D, Novoa-Carballal R, Fernandez-Megia E, Riguera R, *et al*. Hyaluronic acid/chitosan-g-Poly(ethylene glycol) nanoparticles for gene therapy: an application for pDNA and siRNA delivery. Pharm Res. 2010;27:2544–55.
20. Upadhyay KK, Bhatt AN, Mishra AK, Dwarakanath BS, Jain S, Schatz C, *et al*. The intracellular drug delivery and anti tumor activity of doxorubicin loaded poly(γ-benzyl l-glutamate)-b-hyaluronan polymersomes. Biomaterials. 2010;31:2882–92.
21. Carafa M, Di Marzio L, Marianecci C, Cinque B, Lucania G, Kajiwara K, *et al*. Designing novel pH-sensitive non-phospholipid vesicle: characterization and cell interaction. Eur J Pharm Sci. 2006;28:385–93.
22. Hafezand IM, Cullis PR. Cholesteryl hemisuccinate exhibits pH sensitive polymorphic phase behavior. Biochim Biophys Acta (BBA) Biomembr. 2000;1463:107–14.
23. Simões S, Moreira JN, Fonseca C, Düzgüneş N, Pedroso de Lima MC. On the formulation of pH-sensitive liposomes with long circulation times. Adv Drug Deliv Rev. 2004;56:947–65.
24. Naik S, Patel D, Chuttani K, Mishra AK, Misra A. In vitro mechanistic study of cell death and in vivo performance evaluation of RGD grafted PEGylated docetaxel liposomes in breast cancer. Nanomedicine Nanotechnol Biol Med. 2012;8:951–62.
25. Morikawa Y, Koike H, Sekine Y, Matsui H, Shibata Y, Ito K, *et al*. Rapamycin enhances docetaxel-induced cytotoxicity in a androgen-independent prostate cancer xenograft model by survivin downregulation. Biochem Biophys Res Commun. 2012;419:584–9.
26. Kintzel PE, Michaud LB, Lange MK. Docetaxel-associated epiphora. Pharmacother J Hum Pharmacol Drug Ther. 2006;26: 853–67.
27. Danquah MK, Zhang XA, Mahato RI. Extravasation of polymeric nanomedicines across tumor vasculature. Adv Drug Deliv Rev. 2011;63:623–39.
28. Baker J, Ajani J, Scotté F, Winther D, Martin M, Aapro MS, *et al*. Docetaxel-related side effects and their management. Eur J Oncol Nurs. 2009;13:49–59.
29. Bae Y, Nishiyama N, Fukushima S, Koyama H, Yasuhiro M, Kataoka K. Preparation and biological characterization of polymeric micelle drug carriers with intracellular pH-triggered drug release property: tumor permeability, controlled subcellular drug distribution, and enhanced in vivo antitumor efficacy. Bioconjug Chem. 2004;16:122–30.
30. Muthu MS, Rawat MK, Mishra A, Singh S. PLGA nanoparticle formulations of risperidone: preparation and neuropharmacological evaluation. Nanomedicine Nanotechnol Biol Med. 2009;5:323–33.
31. Li N, Zhuang C, Wang M, Sun X, Nie S, Pan W. Liposome coated with low molecular weight chitosan and its potential use in ocular drug delivery. Int J Pharm. 2009;379:131–8.
32. Carafa M, Di Marzio L, Marianecci C, Cinque B, Lucania G, Kajiwara K, *et al*. Designing novel pH-sensitive non-phospholipid vesicle: characterization and cell interaction. Eur J Pharm Sci. 2006;28:385–93.
33. Lavasanifar A, Samuel J, Kwon GS. Poly(ethylene oxide)-block-poly(l-amino acid) micelles for drug delivery. Adv Drug Deliv Rev. 2002;54:169–90.
34. Liu Q, Wu J, Tan T, Zhang L, Chen D, Tian W. Preparation, properties and cytotoxicity evaluation of a biodegradable polyester elastomer composite. Polym Degrad Stab. 2009;94:1427–35.
35. Ungaro F, Conte C, Ostacolo L, Maglio G, Barbieri A, Arra C, *et al*. Core-shell biodegradable nanoassemblies for the passive targeting of docetaxel: features, antiproliferative activity and in vivo toxicity. Nanomedicine Nanotechnol Biol Med. 2012;8:637–46.
36. Peerand D, Margalit R. Loading mitomycin C inside long circulating hyaluronan targeted nano-liposomes increases its antitumor activity in three mice tumor models. Int J Cancer. 2004;108:780–9.
37. Rivkin I, Cohen K, Koffler J, Melikhov D, Peer D, Margalit R. Paclitaxel-clusters coated with hyaluronan as selective tumor-targeted nanovectors. Biomaterials. 2010;31:7106–14.
38. Plattand VM, Szoka FC. Anticancer therapeutics: targeting macromolecules and nanocarriers to hyaluronan or CD44, a hyaluronan receptor. Mol Pharm. 2008;5:474–86.
39. Zhou B, Weigel JA, Fauss L, Weigel PH. Identification of the hyaluronan receptor for endocytosis (HARE). J Biol Chem. 2000;275:37733–41.
40. Cho H-J, Yoon I-S, Yoon HY, Koo H, Jin Y-J, Ko S-H, *et al*. Polyethylene glycol-conjugated hyaluronic acid-ceramide self-assembled nanoparticles for targeted delivery of doxorubicin. Biomaterials. 2012;33:1190–200.